Kinetic Properties of Bursty Bulk Flow Events

Li-Jen Chen,[1,2] D. Larson,[3] R. P. Lin,[3] M. McCarthy,[2] G. K. Parks,[2]

Abstract. Particle distributions of bursty bulk flow (BBF) events in the central plasma sheet regions show that the high earthward velocity comes from a combination of energetic ion flux increases (>few keV) in the earthward direction and decreases of similar energy fluxes in the tailward direction. The energetic ion increases are observed to ~few MeV during intense events, indicating the responsible mechanisms efficiently accelerate particles. The BBF events are intimately tied to the dynamics of tail current sheet reconfiguration and are observed sporadically at all phases of a substorm.

Introduction

The outer edge of the plasma sheet boundary layer (PSBL) in the geomagnetic tail is permeated with intense ion beams propagating along the magnetic field direction (Forbes et al., 1981; Takahashi and Hones, 1988). These ion beams contribute to high velocity moments (>400 km/s) in the earthward direction. Recent observations show that the PSBL also supports unidirectional ion beams propagating in the tailward direction (Parks et al., 1998). These tailward propagating beams are as intense as earthward propagating beams, but their velocity moments are usually small (<200 km/s). Examination of detailed phase space distributions has clarified why this is so. Whereas the plasma distribution of ion beams propagating in the earthward direction is dominated by the beam component, the tailward beam is superposed on another isotropic component, and the combination of the two distributions yield small mean velicities in the tailward direction.

Studies that use plasma bulk parameters consider three variables, the density, mean velocity and mean square velocity. These parameters are obtained from the reduction of the distribution function. To study the physics beyond that provided by the macroscopic variables, the phase space distributions must be examined. A case in point concerns the counter streaming beams of nearly equal intensities at similar speeds that would yield zero mean velocity moments. The bulk parameter studies miss the presence of these beams. However, a considerable amount of information is contained in these beams that can help our understanding of geo-

magnetic tail dynamics.

We have thus extended our studies of the phase space distributions of ions and electrons to the vicinity of the central plasma sheet (CPS). The first results established the CPS region often includes multicomponent plasma distributions including ion and electron beams that likely originate from the current sheet (Chen et al., 1999). We have now extended our studies to identify features of plasma distributions that are responsible for high mean velocities in the CPS region. This article will show that the plasma distributions that contribute to bursty bulk flow events (Angelopoulos et al., 1992) come mainly from the directional anisotropy of high energy ions (>few keV) which extend to ≈MeV energies during intense events.

Observations

The plasma observations of March 27, 1996 are used to illustrate many of the common features that have been observed by the 3D plasma instrument (Lin et al., 1995) on the Wind spacecraft during perigee passes through the near-earth CPS region of the geomagnetic tail. The top three panels of Figure 1 summarize the first three moments of the distribution function obtained during the time interval 10-15 UT (the mean square velocity has been equated to temperature in the third panel). The fourth panel shows the three components of the magnetic field (courtesy of R. Lepping). The bottom two panels are energy spectrograms for fluxes travelling in the sunward and tailward directions. The time resolution of ion measurements is 48s or 24 s and of the magnetic field, 3s. The position of the Wind spacecraft at 1030 UT was $(-14.8, 12.0, -1.4)$ and at 1430 UT $(-15.6, 6.8, 1.1)$ in Earth radii (R_e).

The velocity moments show several events with $\langle V_x \rangle$ that exceed 400 km/s in the earthward direction (second panel). But note that there is also significant $\langle V_y \rangle$. These events have typical durations of ∼10 minutes and the concurrent magnetic field measurements made on Wind indicate weak magnetic fields of the CPS region, except for the event at 1410 UT, which was accompanied by >20 nT $|B_x|$ and a density ∼0.1/cc, indicating properties of the PSBL. These high earthward $\langle V_x \rangle$ are identified with the events studied earlier by Baumjohann et al. (1990) and Angelopoulos et al. (1992), who called them bursty bulk flow (BBF) events.

The sunward energy spectrogram indicates that ion flux increases that contribute to the high $\langle V_x \rangle$ events have typical energies of ∼ 10 keV. An important feature about these events is that significant flux increases are detected to the highest energy channel of the detec-

tor (~27 keV). At the same time, tailward going fluxes decrease from the highest energy channels down to a few keV. This combination of flux increase and decrease of high energy ions in the two opposite directions is the main cause for the high velocity moments.

Figure 2 shows examples of ion distributions for the events that occurred around 1030 and 1430 UT. These plots, in the spacecraft frame, represent 2D slices of the 3D distributions along the plane whose normal is defined by $\mathbf{B}\times\mathbf{V}$, where $\mathbf{V}$ is the mean velocity, with $\hat{B}$ as X-axis and $\hat{V}_\perp$ as Y-axis. The lines are isocontours of phase space densities in $(V_\parallel, V_\perp)$ space. The magnetic elevation and the azimuth angles are shown on the top right and left and the intensity on the lower right. The corresponding 1D cuts of the distributions are shown in the bottom row. Both cuts along ($\times$) and perpendicular ($\diamondsuit$) to the magnetic field are plotted to illustrate the behavior of the low energy and the high energy components. The ion distribution for the 1030 UT event (48 s average) includes a core of anisotropic low energy ions that is elongated along $V_\perp$ and is slightly shifted in the antiparallel direction, and a broad beam covering $\sim 45^\circ$ in pitch-angles along the magnetic field direction at ~900 km/s, ~5 keV. Both the core and the energetic beam are displaced from the origin along $+V_\perp$, indicating the plasmas at this time were being convected (~200 km/s). The 1430 UT distribution (24 s average) shows an extremely hot component that lies along the $V_\perp$ direction. The corresponding perpendicular 1D cut shows a sharp break at ~500 km/s, above which is a plateau that extends out of the scale, and below it is a soft component that extends to the lowest threshold of our detector.

The increase of high energy ion flux extends to the 2.082 MeV channel of the solid state telescopes (SST) as shown in Figure 3, which is a stack plot of omnidirectional ion fluxes of various energies from both the electrostatic analyzer (PESA-H) and SSTs. Figure 4 shows examples of energy spectra from ~70 eV to a few MeV taken before, during and after the 1030 and 1430 UT events. Spectra from 120 angular bins are displayed for PESA-H and 44 for SST. The directions are color-sorted to reveal information on the direction the ions are travelling. The red/black and purple are toward the Sun and the green is antisunward.

The first spectrum is taken from ~1000 UT. There are a low energy component and a high energy component present in the spectrum. The SST shows continuation of the high energy component. We will focus primarily on the directional behavior of the high energy component. Note for the 0959:54 spectra, before

the event, there is little spread indicating the ions are isotropic. For the 1430 UT event, ions from few keV to 2 MeV all display similar directional anisotropy, with sunward flux (red and black) the highest and antisunward (green) the lowest. Similar anisotropy extends from a few keV to 1 MeV for the 1030 UT event. The spreading of these spectral lines occurs because the fluxes at any given energy are highly dependent on the travelling direction of the particles. The 1450:57 spectra, after the events, show isotropy like the spectra before the event, but with larger intensities of energetic particles. Finally, note that the peak of the 1430 UT spectrum lies at the high end of the energy detection threshold (~30 keV) for PESA-H. This incomplete sampling of the ion population indicates the moments calculated from the PESA-H ion distribution underrepresents the actual values of the real population.

Summary and Discussion

The kinetic properties of BBF events revealed by the distribution functions and energy spectra provide important information on the possible generating mechanisms of these events. For the 1030 UT event, the $E \times B$ drift velocity is ~200 km/s, whereas $\langle V_x \rangle$ reaches ~600 km/s. For the 1430 UT event, the soft component does not have the same $V_\perp$ as the hard component, so there is no evidence for the $E \times B$ drift velocity (figure 2). Besides, note that $\partial B/\partial t$ and $\partial^2 B/\partial t^2$ are nonvanishing, that is, there is a time-dependent electric field. Therefore, $E \times B$ drift assuming a time-stationary dawn-dusk electric field is not a good candidate for the generating mechanism of the large $\langle V_x \rangle$.

An important feature of the high velocity moment BBF events in the CPS is that they involve enhancement of energetic ions. Typical energies of these ions are 10 keV, but significant ion flux increases occur to MeV energies. The ion energy spectra show directional dependence with ions > few keV to MeV from the tail representing the major contribution to the velocity moments. This is true for nearly all of the events we have studied (~50 cases) which cover distances from ~ 10-30 R_e in the tail. The energy spectra during the BBF events cannot be obtained by simple shifts of the spectra. A comparison of 1430:51 and 1450:57 spectra shows that for > 200 keV ions, the sunward fluxes of 1430:51 are about 2 orders of magnitude higher, but the tailward fluxes are comparable to the flux level of 1450:57.

The BBF events are closely associated with the tail current sheet reconfiguration. One normally observes the magnetic B_x component decreases dramatically just before a BBF event. The B_z component usually in-

creases, but they are not the usual dipolarizations observed with substorm onsets since here they are accompanied by high frequency magnetic field oscillations in all three components. Moreover, the B_z values exceed what one would expect for the dipole field at that location, suggesting the current sheet disruption (Lui et al., 1992) alone cannot explain the results. (For the 1030 UT event, the dipole field is estimated as $\approx$ 4 nT, but the observed value exceeded 10 nT; for the 1430 UT event, the dipole estimate yields $\approx$ 6 nT, but $B_z \sim$ 15 nT was observed.)

Examination of the relationship to substorms indicates the BBFs occur at all phases of a substorm (not shown). They have rarely been detected at the onset phase and some occur during weak auroral actitvities such as pseudo breakup events (Fillingim et al., 1999). For the events shown in Figure 1, they were observed $\sim$45 minutes (the 1030 UT event), and $\sim$30 minutes (the 1430 UT event) after the onsets. The high $\langle V_x \rangle$ BBF events are correlated with the brightening of the aurora and intensification of the auroral kilometric radation (not shown). The responsible mechanisms in the CPS are thus closely related to the electron distributions which generate the AKR in the ionosphere. Future studies will examine the detailed plasma energy spectra to sort out adiabatic and nonadiabatic features to better identify the mechanisms involved.

Acknowledgments. Research at the Universities of Washington and California at Berkeley is funded in part by NASA grants NAG5-3170 and NAG5-26580.

References

Angelopoulos, V., et al., Bursty bulk flows in the inner central plasma sheet , *J. Geophys. Res.*, *97*, 4027, 1992.

Baumjohann, W., G. Paschmann and H. Luhr, Characteristics of high-speed ion flows in the plasma sheet, *J. Geophys. Res.*, *95*, 3801, 1990.

Chen, Li-Jen, et al., Multicomponent plasma distributions in the tail current cheet, submitted to *Geophys. Res. Lett.*, September, 1999.

Fillingim, M., et al., Coincident Polar/UVI and Wind Observations of Pseudobreakups, submitted to *Geophys. Res. Lett.*, November, 1999.

Forbes, T. et al., Evidence for the tailward retreat of a magnetic neutral line in the magnetotail during substorm recovery, *Geophys. Res. Lett.*, *8*, 261, 1981.

Lin, R. P., et al., A three dimensional plasma and energetic particle investigation for the Wind spacecraft, *Space Sci. Rev.*, *71*, 125, 1995.

Lui, A. T. Y. et al., Current Disruption in the Near Earth Neutral Sheet., *J. Geophys. Res.*, *97*, 1461, 1992.

Parks, G. K., et al., New observations of ion beams in the plasma sheet boundary layer, *Geophys. Res. Lett.*, *25*, 3285, 1998.

Takahashi, K. and E. W. Hones, Jr., ISEE 1 and 2 observations of ion distributions at the plama sheet-tail lobe boundary, *J. Geophys. Res.*, *93*, 8558, 1988.

L. Chen, G. Parks, and M. McCarthy, Geophysics Program, Box 351650, University of Washington, Seattle, WA 98195. (E-mail: lijen@u.washington.edu)

D. Larson and R. P. Lin, Space Science Laboratory, University of California, Berkeley, CA 94720

(Received _____)

[1]Physics Department, University of Washington, Seattle, WA

[2]Geophysics Program, University of Washington, Seattle, WA

[3]Space Science Laboratory, University of California, Berkeley, CA

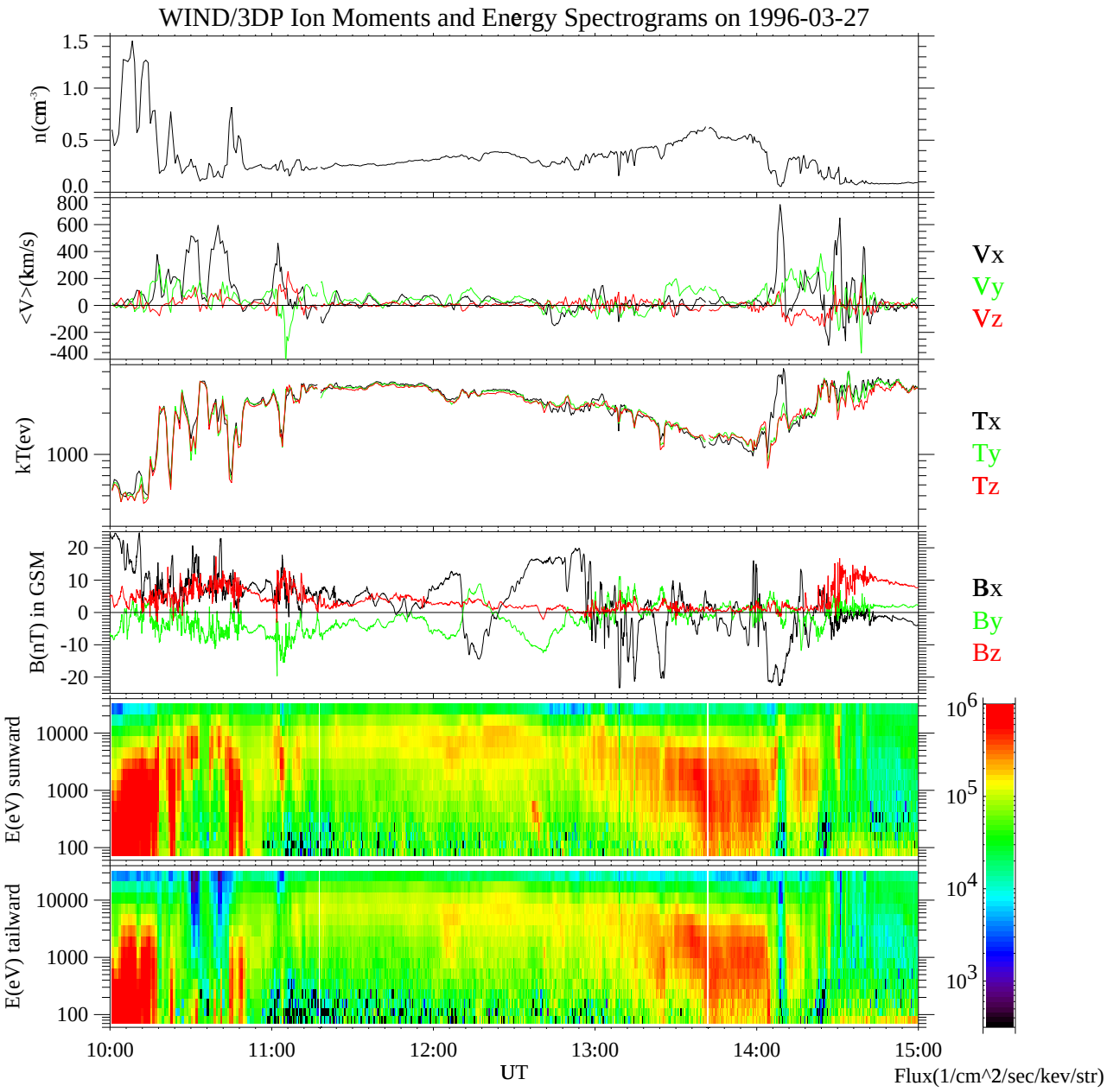

Figure 1. The top three panels show the first three computed moments of the ion distribution function for March 27, 1996. The fourth panel shows the three components of the magnetic field. The bottom two panels show energy-time spectrograms of ions travelling in the sunward and tailward directions.

Figure 1. The top three panels show the first three computed moments of the ion distribution function for March 27, 1996. The fourth panel shows the three components of the magnetic field. The bottom two panels show energy-time spectrograms of ions travelling in the sunward and tailward directions.

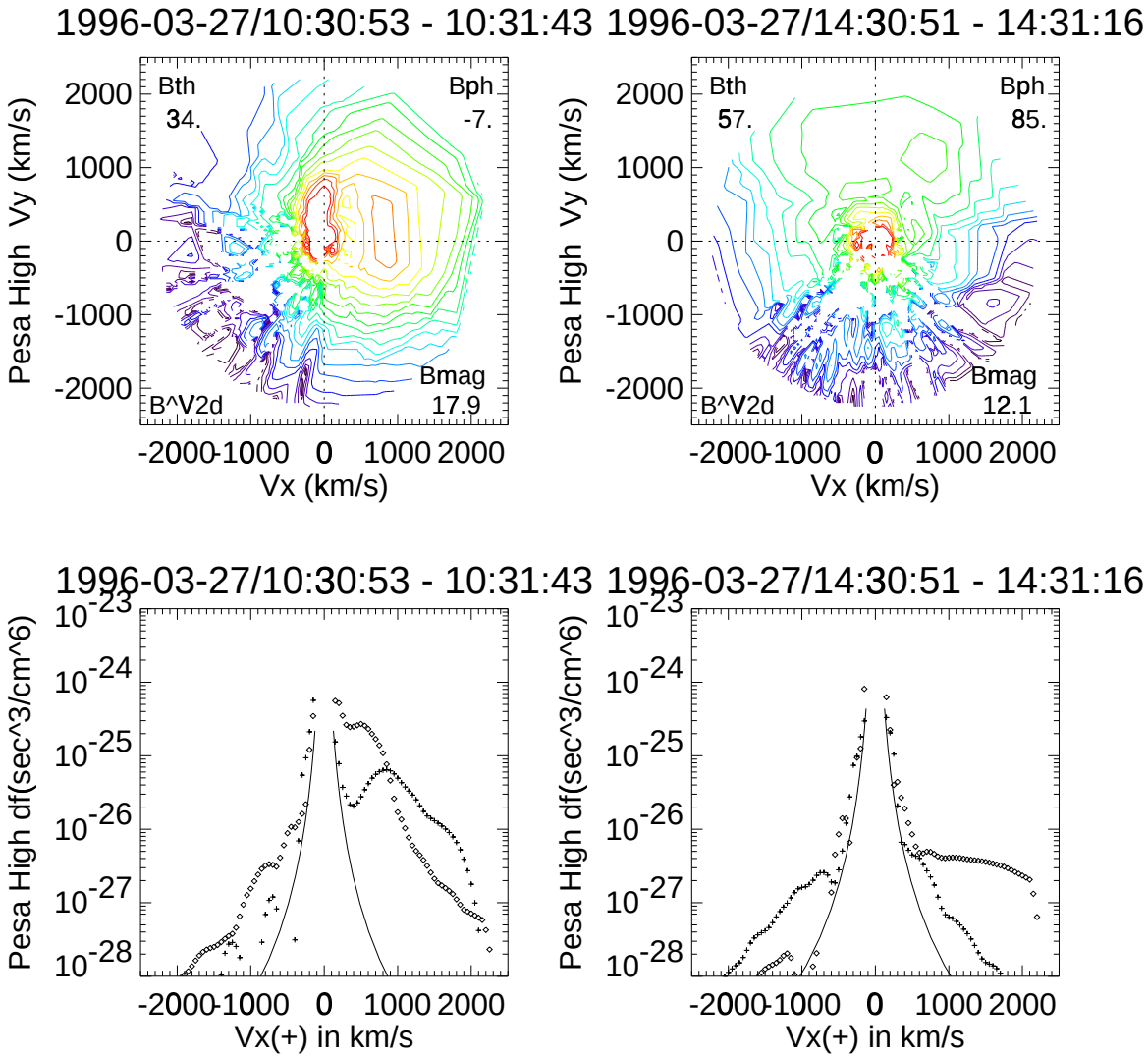

Figure 2. Isocontours of phase space density and 1D cuts of the ion distributions in $(V_{||}, V_{\perp})$ space for the two BBF events(see text for detailed explainations).

Figure 2. Isocontours of phase space density and 1D cuts of the ion distributions in $(V_{||}, V_{\perp})$ space for the two BBF events(see text for detailed explainations).

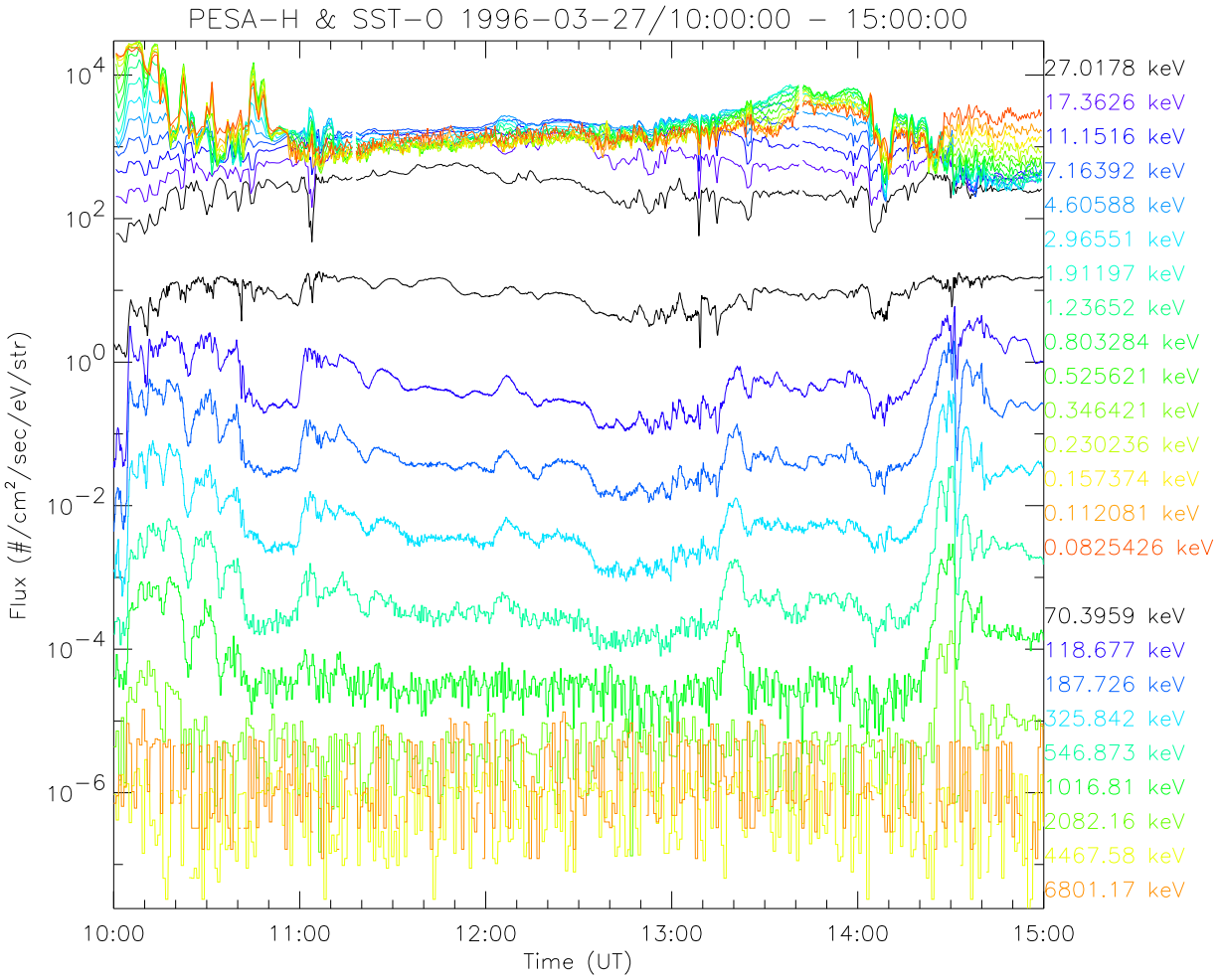

Figure 3. Stack plots of ion fluxes from ∼70 eV to 6.8 MeV. Note the increase of ion fluxes in the 2 MeV channel at 1430 UT during the BBF event.

Figure 3. Stack plots of ion fluxes from ∼70 eV to 6.8 MeV. Note the increase of ion fluxes in the 2 MeV channel at 1430 UT during the BBF event.

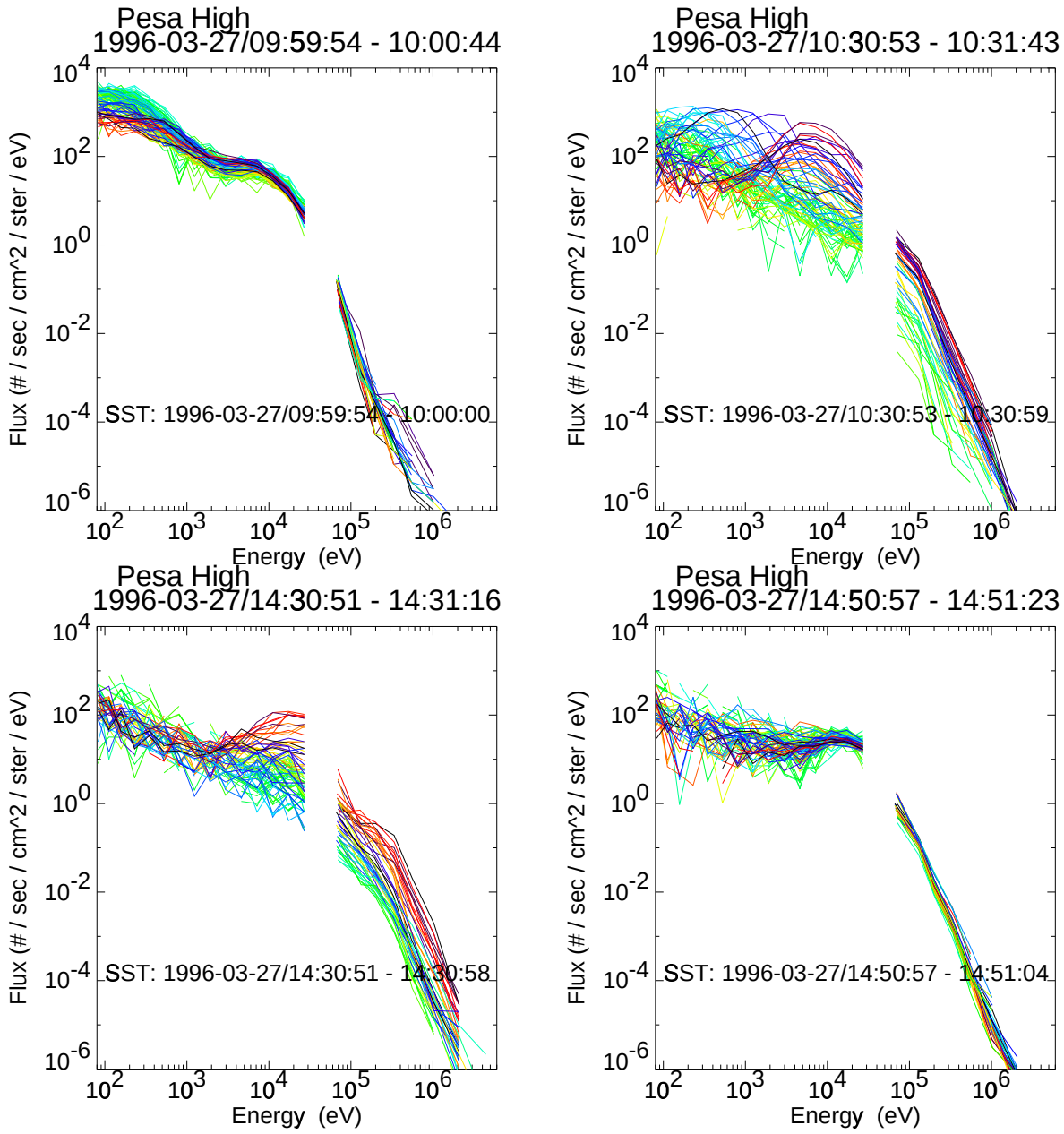

Figure 4. Energy spectra from ~70 eV to several MeV before, during and after two sample BBF events. At 200 keV, there is ~ 16% error due to counting statistics for the angular bin with the largest counts. ~ 11% statistical error in the 2 MeV channel for the angular bin which has the largest counts.

Figure 4. Energy spectra from ~70 eV to several MeV before, during and after two sample BBF events. At 200 keV, there is ~ 16% error due to counting statistics for the angular bin with the largest counts. ~ 11% statistical error in the 2 MeV channel for the angular bin which has the largest counts.

CHEN ET AL.: KINETIC PROPERTIES OF BBF EVENTS

CHEN ET AL.: KINETIC PROPERTIES OF BBF EVENTS

CHEN ET AL.: KINETIC PROPERTIES OF BBF EVENTS

CHEN ET AL.: KINETIC PROPERTIES OF BBF EVENTS

CHEN ET AL.: KINETIC PROPERTIES OF BBF EVENTS

CHEN ET AL.: KINETIC PROPERTIES OF BBF EVENTS

CHEN ET AL.: KINETIC PROPERTIES OF BBF EVENTS

CHEN ET AL.: KINETIC PROPERTIES OF BBF EVENTS

CHEN ET AL.: KINETIC PROPERTIES OF BBF EVENTS

CHEN ET AL.: KINETIC PROPERTIES OF BBF EVENTS

CHEN ET AL.: KINETIC PROPERTIES OF BBF EVENTS

CHEN ET AL.: KINETIC PROPERTIES OF BBF EVENTS

CHEN ET AL.: KINETIC PROPERTIES OF BBF EVENTS

CHEN ET AL.: KINETIC PROPERTIES OF BBF EVENTS

CHEN ET AL.: KINETIC PROPERTIES OF BBF EVENTS

CHEN ET AL.: KINETIC PROPERTIES OF BBF EVENTS

CHEN ET AL.: KINETIC PROPERTIES OF BBF EVENTS